TRANSFERABILITY OF PLANE–STRESS R-CURVES: EFFECTS OF SPECIMEN SIZE AND CRACK LENGTH

V.P. Naumenko*, O. Kolednik♦, N.P. O'Dowd◇, G.S. Volkov* and A.I. Semenets•

A systematic experimental study of the crack-growth resistance of thin-sheet aluminium has been conducted on large- and small-size specimens. The ability of different characterisation parameters such as the J integral and the crack tip opening displacement to describe the fracture resistance at initiation and at steady-state is examined. Strong size effects have been observed, notwithstanding the rather large scatter of the data—the bigger specimens (smaller magnitude of T stress) tending to fail at higher values of J and CTOD. This suggests that fracture toughness under a ductile mechanism decreases with a decrease in constraint. This is in contrast to fracture via a cleavage mechanism which has been observed to show the opposite trend.

INTRODUCTION

Fracture toughness and crack-extension resistance of metallic materials are most often expressed in terms of the stress intensity factor, K, the J-integral, J, the crack-tip opening displacement, V, (usually termed CTOD) the crack-tip opening spacing, δ, and the crack-tip opening angle, α. These crack-driving parameters provide the basis for the most easily available methods used in one-parameter characterisation of Mode I fracture resistance.

In this paper, the fracture of thin sheet aluminium is examined. The fracture resistance, K_R, is determined using ASTM Standard Practice E 561-92a (1). The fracture toughness in terms of J has also been obtained, using a number of procedures, the EPRI scheme (2), the GTP method (3) and the ETM method (4). (The latter method is essentially equivalent to ASTM E561-92A though fracture toughness is phrased in terms of J rather than K.) Common to these procedures is a tacit

* Department of Modelling and Fracture Mechanics, Institute for Problems of Strength, Kyiv, Ukraine.
♦ Erich Schmid Institute for Solid State Physics, Austrian Academy of Sciences, Leoben, Austria.
◇ Department of Mechanical Engineering, Imperial College of Science and Technology, UK.
• Antonov Design Bureau, Kyiv, Ukraine

assumption that the influence of the in-plane size and original crack length on fracture resistance is negligible, as long as the requirements of ASTM E 561-92a are met. Recent work of Dadkhah and Kobayashi (5) has shown that the displacement fields surrounding a stably growing crack in a thin aluminium plate may differ widely from the displacement fields given by the HRR distribution (Rice and Rosengren, (6), Hutchinson, (7)) or the J-Q field (O'Dowd and Shih (8)). Therefore, the use of J or a two parameter J-Q approach may not be valid in characterizing fracture for growing cracks under plane stress conditions. In this work, fracture resistance of thin aluminium plate of different size and crack length to specimen width ratio is examined and the ability of the cited methods (1-4) to describe the fracture behaviour is assessed.

MATERIALS TESTING

The test material is a high-strength aero-skin aluminum 1163 AT in the as-received condition (similar to Al 2024-T351). Standard sheet-type specimens and cracked specimens of 1.05 mm thickness were made such that the applied stress, σ, was parallel to the rolling direction. The tensile properties of the material under ambient conditions are: elastic modulus E = 73 GPa, 0.2% offset yield stress σ_Y = 335 MPa, and the ultimate strength σ_u = 445 MPa. The stress-strain curve averaged over seven replicate tests was well approximated by the Ramberg-Osgood material law: $\varepsilon/\varepsilon_O = \sigma/\sigma_O + \lambda(\sigma/\sigma_O)^n$, with $\sigma_O = \sigma_Y$, $\varepsilon_O = \sigma_O/E$, $\lambda = 1.2$ and $n = 11$.

The specimen configuration, dimensions and procedures for fatigue precracking and subsequent testing, met the requirements of ASTM E561-92a. In this paper, results from tests carried out on large center cracked tension (M(T)) specimens of width $2W$ = 1200 mm and tests of small-size specimens, $2W$ = 120 mm are presented. To eliminate uncontrolled or spurious stress distribution in the specimens, rigid face plates with teflon-liner sheets were affixed to each specimen. In the course of the tests the specimens were loaded incrementally, allowing time between steps for the crack to stabilise before measuring the load, P. In addition, once the crack had stabilised a close-up photograph of the near crack-tip profile was taken allowing the amount of crack growth, Δc and crack tip opening, δ, to be determined. More than fifteen steps for each test condition were measured for each R-curve.

EXPERIMENTAL RESULTS

For uniformity of analysis a continuous fit to the R – curve was determined using

$$R = A_0 + A_1(\Delta c) + A_2(\Delta c)^2 \quad \text{.....(1)}$$

where R is any of the crack characterising parameters, R (K_R, J_R, V_R, δ_R or α_R). To determine K_R, J_R, V_R the procedure of crack modelling of Naumenko (9) was used whereby $2a = 2c_u$, where $2a$ is the length of a mathematical cut and $2c_u$ is the length of the actual crack in the undeformed specimen. The average values of the different fracture parameters are summarised in Tables 1 to 4. The J integral was evaluated using a number of different procedures: the GTP procedure (4) which combines the

elastic part of J, J^{el}, with the plastic part obtained from the area under the load displacement curve; the EPRI procedure (2) which uses a modified elastic J in conjunction with a power law expression for the plastic part of J; and the ETM procedure (3) which is essentially the ASTM K value converted to J via the plane stress small scale yielding relation, $J = K^2/E$. Fracture initiation was taken to correspond to Δc = 0.2 mm as determined from Eq (1). It may be seen from Table 1 that the different J estimates show considerable variation, in particular the GTP method for the small, shallow crack specimen. This may be because the expression used here is strictly valid only for deep cracks (10).

TABLE 1 – Mean K and J estimates at initiation (Δc = 0.2 mm).

$2a_{tt}$ (mm)	a/W	$K^{ASTM}_{0.2}$ (Mpa $m^{1/2}$) (1)	$J^{el}_{0.2}$ (kJ/m^2) (4)	$J^{GTP}_{0.2}$ (kJ/m^2) (4)	$J^{EPRI}_{0.2}$ (kJ/m^2) (2)	$J^{ETM}_{0.2}$ (kJ/m^2) (3)
Small–Size Specimens						
12.4	0.10	53.3	23.8	157.8	59.0	38.9
30.3	0.25	61.9	40.3	73.9	65.8	52.6
48.2	0.40	67.4	49.3	80.5	74.8	62.3
Large –Size Specimens						
95.0	0.08	61.1	47.0	59.8	43.6	51.4
157.3	0.13	82.4	82.4	91.6	86.7	93.4
332.7	0.28	80.0	82.7	79.6	80.9	86.9
514.4	0.43	96.1	118.1	120.9	120.1	122.3

The variation of J from the EPRI procedure with specimen size is plotted in Fig. 1, the scatter in the data is indicated by the error bars. In Table 2, values of the crack tip opening displacement, V determined from the relationship, $V = d_n(J/\sigma_Y)$ are given, where for EPRI (2) d_n = 0.76 and for the ETM procedure (3) d_n = 1.0.

TABLE 2 – Mean crack opening displacements and angle at fracture initiation.

a/W	$V^{EPRI}_{0.2}$ (mm)	$V^{ETM}_{0.2}$ (mm)	$\delta^{UM}_{0.2}$ (mm)	$\alpha^{UM}_{0.2}$ (rad)
Small–Size Specimens				
0.10	0.13	0.12	0.14	0.026
0.25	0.16	0.16	0.12	0.027
0.40	0.17	0.19	0.15	0.037
Large –Size Specimens				
0.08	0.10	0.15	0.08	0.022
0.13	0.19	0.28	0.18	0.025
0.28	0.18	0.26	0.17	0.019
0.43	0.27	0.36	0.16	0.037

The measured crack tip opening is also included, here given the symbol, δ_R^{UM}. The latter represents the crack opening spacing at various distances, x, from the original crack tip and extrapolated to $x = 0$ (9). This value includes the initial crack-tip spacing, δ_i, (typically 0.01–0.04 mm for these tests) and thus is the total crack opening. Crack-tip constraint parameters are given in Table 3. The quantities $T_{0.2}$ and $Q_{0.2}$ are obtained from Leevers and Radon (11) and O'Dowd et al. (12) respectively, the subscript 0.2 again emphasising that the quantities are evaluated when the amount of crack growth, $\Delta c = 0.2$ mm.

TABLE 3 - Other characterising quantities relevant to fracture initiation.

a/W	$\sigma_{0.2}/\sigma_Y$	$r_{0.2}/\sigma_Y$	$T_{0.2}/\sigma_Y$	$\log(J_{0.2}/a\sigma_Y)$	$Q_{0.2}$ (plane stress)	$Q_{0.2}$ (plane strain)
0.10	0.87	0.65	− 0.88	− 1.55	− 0.07	−1.1
0.25	0.67	0.36	− 0.73	− 1.89	− 0.05	−1.0
0.40	0.54	0.27	− 0.66	− 2.04	− 0.06	−1.0
0.08	0.46	0.11	− 0.44	− 2.56	− 0.02	−0.50
0.13	0.46	0.12	− 0.46	− 2.48	− 0.02	−0.55
0.28	0.30	0.05	− 0.32	− 2.84	− 0.02	−0.40
0.43	0.27	0.05	− 0.32	− 2.86	− 0.02	−0.40

The K_R-curves for several small specimens are shown in Fig 2. The arrows indicate the upper points on the K_R curves, where the net section stress, σ_N, is less then the yield strength of the material (thus these data are invalid under ASTM E 561-92a). The crack approaches steady state when $\Delta c > 3B$, where B is the specimen thickness.

TABLE 4 - Crack resistance after initiation[a] and at steady-state crack growth[b].

a/W	$\left(\frac{dJ_R^{GTP}}{da}\right)_i$	$\left(\frac{d\delta_R^{UM}}{dc}\right)_i$	$\left(\frac{dK_R}{da}\right)_i$	K_s	$\frac{K_S - K_S^{el}}{K_S}$
	(MJ/m^3)		(MPa m$^{-0.5}$)	(MPa m$^{0.5}$)	%
0.10	86.0	0.17	8.74	73.7	28
0.25	70.0	0.20	16.53	94.1	32
0.40	55.2	0.18	34.85	107.5	38
0.08	154.6	0.32	36.00	106.9	13
0.13	68.3	0.19	21.30	127.7	12
0.28	43.8	0.13	15.44	117.9	7
0.43	40.0	0.12	12.10	127.6	7

[a] Crack initiation is defined here as $\Delta c = 0$ and labelled by a subscript "i".

[b] The steady-state condition is defined as $\Delta c = 3B$ and labelled by a subscript "s"

DISCUSSION

It may be noted that the large specimens deform predominately elastically. This is reflected in the low value of $\sigma_{0.2} / \sigma_Y$ and $r_{0.2} / \sigma_Y$ in Table 3 ($\sigma_{0.2}$ and $r_{0.2}$ are the remote stress and plastic zone size at initiation, respectively) and the small difference between J^{el} and the total J in Table 1. The smaller specimens however show significant levels of plasticity, though in all cases yielding is contained. Because of the large scatter in the data, it is difficult to make definitive judgements. However, Table 1 and Fig. 1 suggest that the fracture toughness at initiation as measured by J increases with specimen size. This is true for all estimates of J apart from the shallow crack GTP estimate, which as we have stated may be in error. A similar trend is observed for the value of steady state toughness, K_S, in Table 4, i.e. on average K_S is larger for the larger specimens.

While the T stress at fracture varies considerably for the different size specimens, the variation of the constraint parameter Q is much weaker (if plane stress conditions are considered). If indeed plane stress conditions prevail through the thickness of the specimen, then the dependence on specimen size cannot be explained simply via a two parameter J-Q approach. If it is assumed that there is local plane strain behaviour at the crack tip then the results suggest that fracture toughness *increases* with increasing constraint. While the opposite behaviour has been seen in many materials, it may be explained through a consideration of the crack tip opening displacement. As shown in (8), CTOD decreases with increasing constraint. Therefore if fracture initiation is controlled by a critical CTOD, a material constant, low constraint specimens, i.e. small specimens, will show lower initiation toughness and resistance to fracture. Support for this approach is provided by the measured CTOD in Table 2, which shows that CTOD is relatively independent of size.

CONCLUSIONS

Preliminary results for crack growth resistance of aluminium sheet are presented. Our results show that J at initiation and the associated R-curves, depend significantly on the allowable (in ASTM E561-92a) variations of the original crack length and specimen size. The data appear to show an increase in toughness as measured by J with increasing constraint, (using either the elastic T stress or plane strain Q values).

ACKNOWLEDGEMENTS

The authors acknowledge the financial support of INTAS (Project Nr 94-0722) and the Austrian Academy of Sciences for funding the visits of NPOD, VPN and AIS to Leoben. The assistance of G.I. Hanin of the Antonov Design Bureau, Ukraine, is gratefully acknowledged.

REFERENCES

(1) ASTM Standard Practice for R-Curve Determination (E561-92a), Annual Book of ASTM Standards, Vol. 03.01., 1992, pp. 600-611.

(2) Kumar, V., German, M.D., and Shih, C.F., Topical Report No. EPRI NP-1931, RP 1237-1, General Electric, Schenectady, NY., 1981.

(3) Schwalbe, K.-H., Cornec, A., and Heerens, J., in Defect Assessment in Components–Fundamentals and Applications, J.G. Blauel and K.-H. Schwalbe, Eds., Mechanical Engineering Publications Limited, London, 1991.

(4) Schwalbe, K.-H. and Neale, B., Fatigue Fract. Eng. Mater. Struct., Vol. 18, 1995, pp. 413.

(5) Dadkhah, M. S. and Kobayashi, A.S., Fracture Mechanics: 24th Volume, ASTM STP 1207, J. D. Landes, D.E. McCabe, and J.A.M. Boulet, Eds., ASTM, 1994, pp. 48-61.

(6) Rice, J. R. and Rosengren, G.F., J. Mechs. Phys. Solids, Vol. 16, 1968, pp. 1-12

(7) Hutchinson, J. W., J. Mechs. Phys. Solids, Vol. 16, 1968, pp. 13-31.

(8) O'Dowd, N. P. and Shih, C. F. J. Mechs. Phys. Solids, Vol. 39, 1991, pp. 989.

(9) Naumenko, V.P., Proceedings of the Symposium,"Risk and Evaluation on Failure and Malfunction of Systems", E & F.N. Spon and Chapman & Hall, 1996.

(10) Rice, J.R., Paris, P.C. and Merkle, J.G. ASTM STP 536, American Society for Testing of Materials, 1973, pp 231-245.

(11) Leevers, P.S. and Radon J.C., Int. J. of Fracture, Vol. 19, 1982, pp. 311-325.

(12) O'Dowd, N.P., Kolednik, O. and Naumenko, V.P., Submitted for publication.

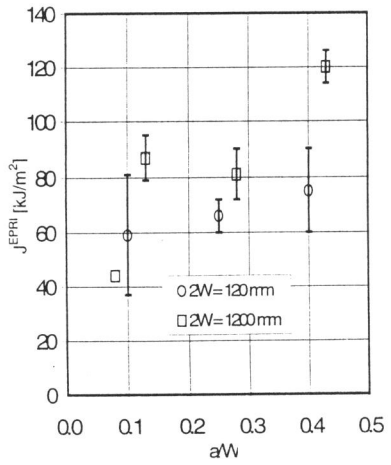

Figure 1, J at initiation using EPRI solutions

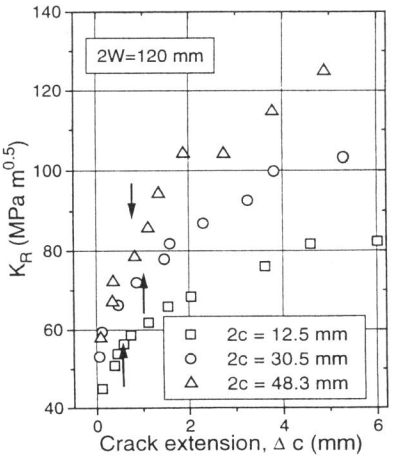

Figure 2, K_R curves for small specimens